RSC Advances

PAPER

View Article Online
View Journal | View Issue

Cite this: *RSC Adv.*, 2017, **7**, 40940

High-power current and fatigue sustainable circuits prepared using low-temperature spray pyrolyzed submicron silver particles

Chi-Nan Cheng,[a] Rong-Ting Liou,[a] Jenn-Ming Song *[a] and Shao-Ju Shih[b]

Silver acetate instead of silver nitrate was used as the precursor to synthesize submicron-sized Ag particles (Ag SMPs) using a thermal-spray pyrolysis method at relatively low processing temperatures. Pastes comprised of Ag particles were produced and sintered at 100 °C or 250 °C to form conductive circuits for different-level microelectronics. The produced circuits were designed for application as interconnections in consumer and automotive devices. The critical current necessary to fuse the circuit was measured to evaluate the interconnect reliability under high-power electrical current stress. The experimental results show that a critical calcination temperature exists between 350 to 400 °C for full silver acetate conversion into Ag powders. The amount of residual precursor, morphology, constituent and size of the Ag particles, as well as the electrical conductance of the sintered structures are all influencing factors. When subjected to heating at 100 °C for 10 min, the sintered conductive Ag SMP lines can withstand current stress density exceeding 1 mA μm^{-2} under 12 V, indicating superior electrical reliability. The low-temperature sintered SMP deposits also demonstrated excellent bending fatigue resistance.

Received 14th June 2017
Accepted 9th August 2017

DOI: 10.1039/c7ra06636h

rsc.li/rsc-advances

1. Introduction

Silver is known for its superior electrical conductivity, thermal conductivity, catalytic property and antibacterial activity. Silver particles have therefore been used for various applications including conductors, electrical contacts, catalysts, wound dressing and so forth.[1]

Ultrasonic spray pyrolysis (SP) has been developed to fabricate fine metallic powders because of its low cost, one-step continuous processing, high purity and chemistry flexibility.[2,3] It is also recognized as an energy-efficient solution based method wherein high frequency ultrasound passes through a liquid precursor solution and forms an aerosol of micron-sized droplets, which are carried by gas flow into a heated zone where solvent evaporation and reactions occur.[3] Table 1 tabulates previous studies about the spray pyrolysis of Ag particles.[4–10] $AgNO_3$ (silver nitrate), Ag_2CO_3, Ag_2O and $AgC_2H_3O_2$ (silver acetate) have been used as precursors. As indicated, calcination temperatures are set to range from 400 °C to 1000 °C according to the precursors, the solvents and the atmosphere. No data of the electrical conductance of sintered structure of the pyrolyzed Ag particles are available. In addition to solid particles with nanosizes or submicron-sizes,[4–6,9,10] fine Ag particles with mesoporous[7,8] or alloyed structure[11–13] can also be synthesized using this method. Ag based composite particles with glasses or oxides have been applied in antibiotics and surface enhanced Raman scattering.[14–16]

To prevent particle coarsening and oxidation at elevated temperatures, silver acetate, with a lower decomposition temperature has been recently chosen to replace the most commonly used precursor, silver nitrate.[10] Fig. 1 shows concise data about the decomposition of two aforementioned silver salts, the dissociation of silver acetate starts from 200 °C to 265 °C, while that of silver nitrate is from 370 °C to 460 °C. However, the literature suggests that a calcination temperature

Table 1 Relevant reports of spray pyrolysis of Ag particles

Precursor	Calcination temperature without residual precursors (°C)	Atmosphere	Electrical resistance of sintered structure	Ref.
$AgNO_3$	600–1000	N_2	N.A.	4
$AgNO_3$	400–800	$N_2 + H_2$	N.A.	5
$AgNO_3$	790	Air	N.A.	6
$AgNO_3$	700	N_2	N.A.	7
Ag_2CO_3	640	Air	N.A.	8
Ag_2CO_3 Ag_2O[a]	400	N_2	N.A.	9
$AgC_2H_3O_2$	400–800	Air	N.A.	10

[a] NH_4OH as the solvent.

[a]Department of Materials Science and Engineering, National Chung Hsing University, Taichung, Taiwan. E-mail: samsong@nchu.edu.tw
[b]Department of Materials Science and Engineering, National Taiwan University of Science and Technology, Taipei 106, Taiwan

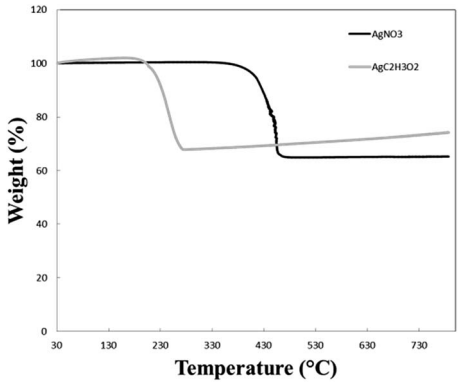

Fig. 1 Weight change of silver salts ($AgNO_3$ and $AgC_2H_3O_2$) upon heating (heating rate: 5 °C min^{-1}).

of 600 °C and above is still needed for the complete decomposition of silver acetate in air.[10] For the particles treated at 400 and 600 °C, a bimodal distribution (nanometer size and submicrometer size) could be found, while the particles treated at 800 °C exhibited a normal distribution (submicron size only).

Using silver acetate as the precursor, this study develops interconnect materials for different level packaging using thermal spray pyrolysis. In consideration for saving energy, the pyrolysis temperature was lowered to range from 250 °C to 500 °C. In order to prepare interconnections for polymeric substrate or repair PCB (printed circuit board) circuits, the particle sintering temperature was reduced to 100 °C. High power current stress and bending fatigue tests for the interconnection were carried out to evaluate the interconnection reliability.

2. Experimental procedures

Silver acetate precursor (99%, $AgC_2H_3O_2$, Alfa Aesar, US) was used to prepare silver particles using a laboratory-scale spray pyrolysis (SP) electrostatic deposition system (Fig. 2). In the SP process, the precursor aqueous solution (0.06 M) was first atomized into fine droplets using an ultrasonic nebulizer at 1.65 MHz. Air flow with a controlled flow rate carried the droplets into the heated tubular reactor with three zones; pre-heating, calcination and post-heating in sequence. In the calcination zone, four temperatures, 250, 300, 350, 400 and 500 °C were chosen and the samples obtained were designated as AgA250 to AgA500 respectively. The

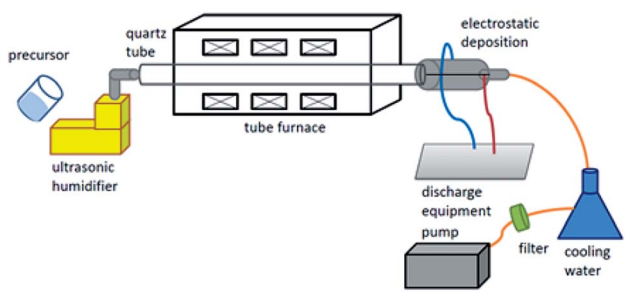

Fig. 2 Schematic view of spray pyrolysis system.

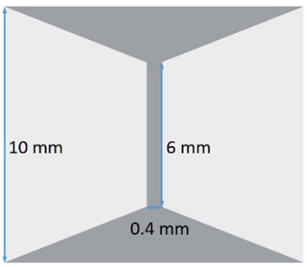

Fig. 3 The pattern on Si chips for the electrical current stress test.

pre-heating and post-heating temperature zones were set 50 to 250 °C below the calcination temperature. The droplets in the reactor underwent solvent evaporation, solute precipitation, precursor decomposition and conversion into Ag particles. The resulting powders were then collected using a cylindrical electrostatic collector with an applied high-voltage potential of −16 kV. For comparison, spray pyrolysis of Ag particles using silver nitrate as the precursor were also prepared with selected calcination temperature and named as AgN.

The thus formed powders were characterized using TGA (thermogravimetric analysis), X-ray diffractometer, and FTIR (Fourier transform infrared spectroscopy). Ag pastes were prepared by mixing Ag particles and α-terpineol. Ethyl cellulose was added to thicken the pastes. Isothermal heat treatments of the pastes were performed at 100 °C for 10 min or 250 °C for 30 min to simulate different-level interconnect manufacturing processes. Commercial sinter pastes (α-metal Argomax2020) comprised of Ag nanoparticles with an average diameter of 20 nm were adopted for comparison.

The electrical properties of the sintered powders were measured using the four-point method. The current stress test was carried out using the pattern on Si chips sketched in Fig. 3, where the pastes were printed onto the dark gray area. Considering that laptops and automotive electronics run on 12 V electric current, a constant voltage of 12 V was conducted through the stripe connecting the two trapezoid pads, which had a length of 6 mm and width of 0.4 mm.

The fatigue performance of the sintered Ag films on the PET (polyethylene terephthalate) substrate was evaluated using the cyclic bending fatigue test. The cyclic bending test was carried out at a frequency of 2 Hz for 10 000 cycles. The electrical resistivity corresponding to the bending cyclic number was recorded. The outer bending radius of the PET film (R) was 4.5 mm, which was obtained according to the following equations.[17]

$$R = \frac{L}{2\pi}\sqrt{\frac{dL}{L} - \frac{\pi^2 h^2}{12L^2}}$$

where L, dL/L and h denote the initial length, the applied strain and the substrate thickness, respectively.

3. Results and discussion

3.1 Microstructural feature of the thermal-sprayed Ag SMPs

Fig. 4 shows the morphologies of the thermal-sprayed Ag powders. Critical calcination temperature exists for the change

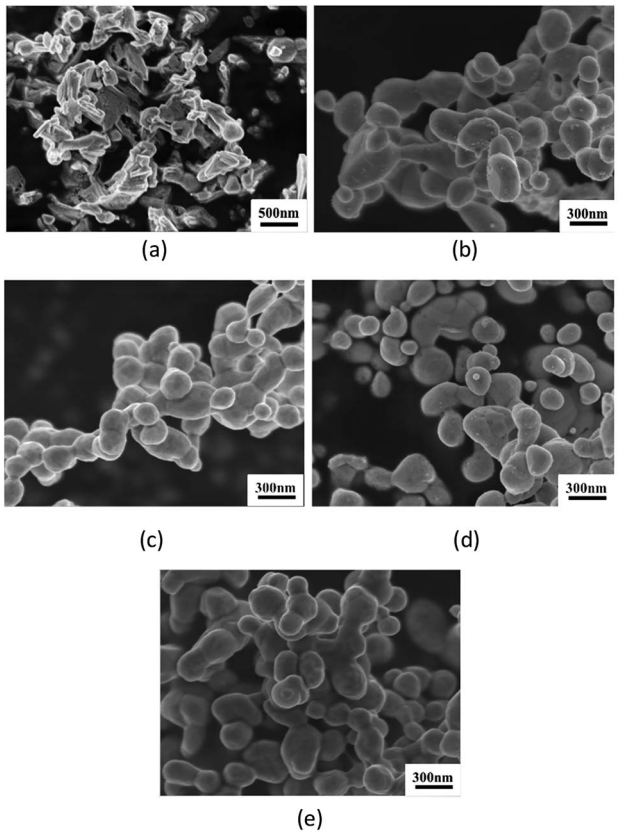

Fig. 4 Ag powders subjected to spray pyrolysis at different temperatures: (a) 250 °C, (b) 300 °C, (c) 350 °C, (d) 400 °C and (e) 500 °C.

in the appearance and constituents of the particles. The morphological difference between AgA250 and the others can be clearly observed. Subjected to calcination at 250 °C, the silver acetate crystals can be distinguished. With a higher heating temperature at 300 °C and above, the particles became rounder and with similar appearances. Average particle size was about 280 nm for 300 °C-calcined samples, while those for the samples calcined at higher temperatures ranged from 240 nm to 255 nm with large data fluctuations. XRD patterns given in Fig. 5 indicate that Ag signals could be observed in all samples and increased with a higher calcination temperature. The diffraction peaks representing $AgC_2H_3O_2$ could only be detected for those samples calcined at 250 °C. Further analyses to clarify the differences caused by calcination temperature are given as follows.

The FTIR results illustrated in Fig. 6 reveal that at 400 °C and above CO_2^- ligands at 1300–1700 cm^{-1} (ref. 18) completely diminished. Thermogravimetric analytic data reveal more information about the residual salts. Fig. 7 displays a decrease in weight for those calcined at 350 °C or below can be clearly seen upon heating. As shown in those curves, the reduction in weight stopped at about 250 °C. The residual $AgC_2H_3O_2$ content for each condition can also be obtained from the TGA curves, *i.e.* 28.1 wt% for the powders calcined at 250 °C, 6.9 wt% for 300 °C and 2.3 wt% for 350 °C. For the powders calcined at 400 °C and 500 °C, the thermal-sprayed powder weight remained unchanged upon heating. The above results

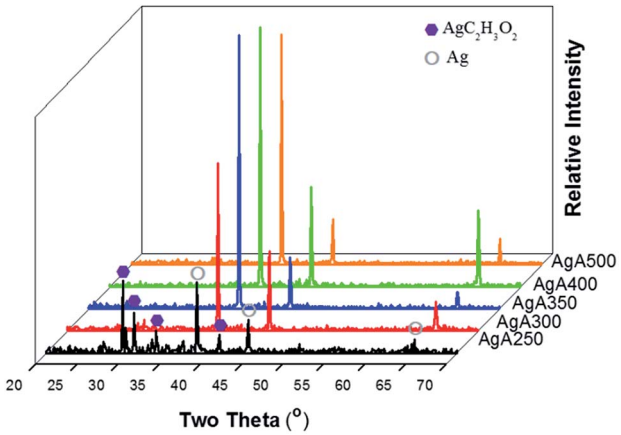

Fig. 5 X-ray diffraction patterns of the Ag powders.

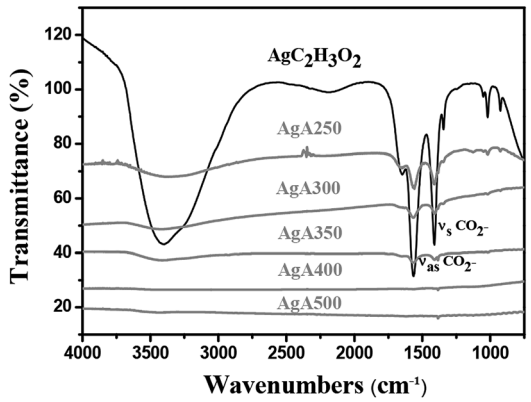

Fig. 6 FTIR spectra of the Ag powders.

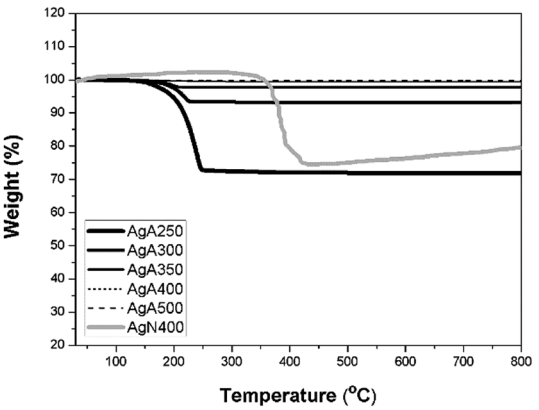

Fig. 7 TGA curves upon heating (heating rate: 5 °C min^{-1}).

demonstrate that a critical pyrolysis temperature exists between 350 °C and 400 °C for the complete decomposition of silver acetate, which was much lower than the reported values in the literature except for those calcined in a reductive atmosphere.[5,9] TGA measurement of the powders made from $AgNO_3$ (AgN400) were also performed for comparison (Fig. 7). It can be found subjected to calcination at 400 °C, AgN400 shows a significant

weight decrease upon heating, which can be ascribed a certain amount of undecomposed precursors.

3.2 Electrical performance of sintered Ag SMPs

In order to fabricate interconnections, Ag pastes were prepared by mixing Ag powders, solvent (α-terpineol) and thickener (ethylcellulose). As illustrated in Fig. 8, it can be clearly seen that electrical resistivity of the sintered structure under all heating conditions decreased significantly with the increase in calcination temperature. 350 °C was a turning point for the resistivity from descending to becoming constant. With respect to the ethylcellulose-thickened pastes subjected to isothermal heating at 250 °C for 30 min, the electrical resistivity as a function of calcination temperature was 61 μΩ cm (250 °C), 64 μΩ cm (300 °C), 25 μΩ cm (350 °C), 16 μΩ cm (400 °C) and 14 μΩ cm (500 °C). The last three data were comparable or even lower than the resistivity of commercial nano-Ag pastes cured at 250 °C (27.3 μΩ cm). The addition of ethylcellulose absolutely played an important role in improving the electrical conductance through the sintered structure densification. It is interesting that when the same pastes were cured at 100 °C for 10 min, the resistivity did not increase too much. For those with the calcination temperature of 350 °C or above, the resistivity was no higher than 100 μΩ cm (*i.e.* 78.7 μΩ cm for 350 °C, 71.6 μΩ cm for 400 °C, and 56.6 μΩ cm for 500 °C). If we replace AgA400 by AgN400, the electrical conductance of 100 °C-heated deposits was undetectable. In comparison to the nano-Ag pastes cured at 100 °C ($\rho = 209$ μΩ cm), this indicates the likelihood for low temperature fabrication of conductive circuits without using costly Ag nanoparticles.

Fig. 9 illustrates the sintered structures of the pastes comprised of AgA400 submicron particles and nano-Ag pastes subjected to heating at different temperatures. By comparison, it can be identified that the sintered structures of Ag submicron particles after heating at 100 °C for 10 min (Fig. 9(a)) or 250 °C for 30 min (Fig. 9(b)) did not differ too much. Both of them still revealed submicron grain size and necking at localized regions.

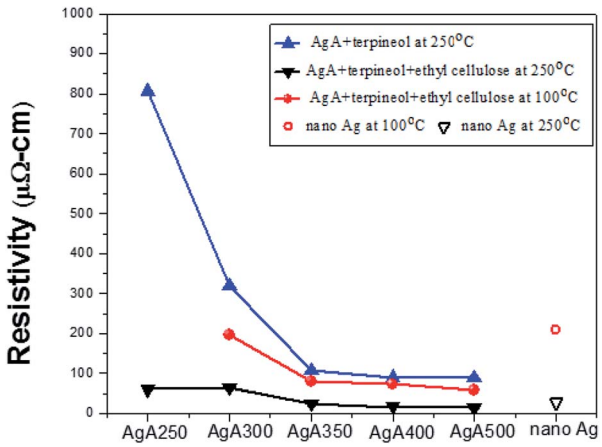

Fig. 8 Electrical resistivities of the sintered structures from Ag SMPs synthesized at different calcination temperatures (those using commercial nano-Ag pastes were given for comparison).

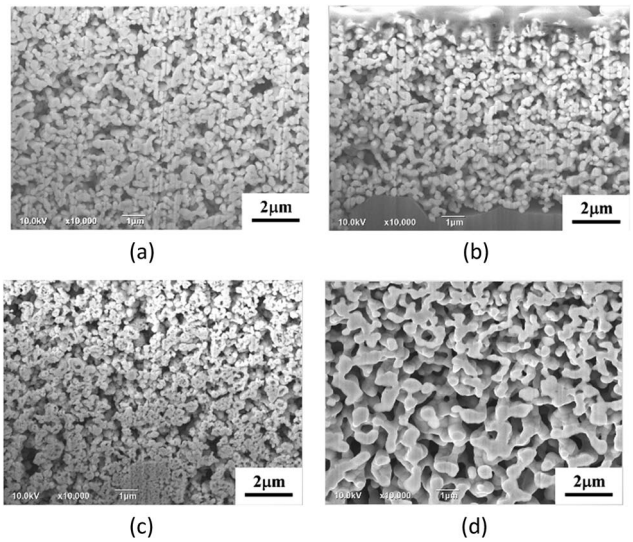

Fig. 9 Cross-sectioned structure of the heat-treated deposits: (a) AgA400 after being heated at 100 °C for 10 min, (b) A400 subjected to heating at 250 °C for 30 min, (c) nano-Ag after being heated at 100 °C for 10 min, and (d) nano-Ag at 250 °C for 30 min.

In contrast, Ag nanoparticles coalesced at 100 °C (Fig. 9(c)) and grew further to micron-size while heated at 250 °C (Fig. 9(d)). It is remarkable that the sintered structure shown in Fig. 9(d) (nano-Ag heated at 250 °C) was much coarser than that in Fig. 9(b) (AgA400 heated at 250 °C). This can explain the drastic decrease in electrical resistivity of nano-Ag when the heating temperature was increased from 100 °C to 250 °C. It can be considered that 250 °C is enough for a more complete surfactant desorption for nano-Ag. The stacking of nano-sized particle deposits was much denser than that of submicron-sized particles; thereby the sintering and linking among the particles were more complete. The partially-sintered structure of AgA400, which was free of organic surfactants, still exhibited excellent electrical conductance.

With respect to the capability to endure high-power electrical current, Fig. 10 indicates that all the Ag SMP pastes subjected to heating at both 100 °C and 250 °C could withstand stress current density exceeding 1 mA μm^{-2} under a constant voltage of 12 V, except those with calcination temperature of 250 °C. The performance was at the same level of nano-Ag sintered conductive tracks cured at 250 °C. As for the lower critical current of 100 °C cured nano-Ag pastes (0.62 mA μm^{-2}), the non-decomposed surfactants in the nanoparticles may account for that. Unlike the electrical or electromigration of nano-metal sintered structures studied in previous reports,[19,20] the failure mechanism in this high-power electrical stress was melting of the Ag conductive lines.

3.3 Bending fatigue reliability of low-temperature sintered Ag SMPs on PET

As illustrated in Fig. 11, it can be clearly seen that the electrical resistivity of the sintered AgA400 structure subjected to curing at 100 °C for 10 min was 35 μΩ cm, much lower than 240 μΩ cm,

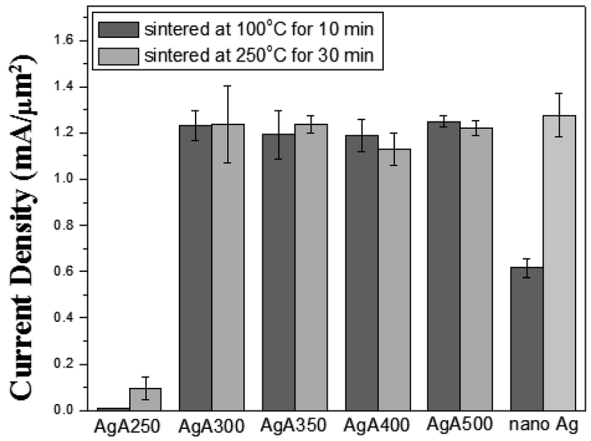

Fig. 10 Critical current density necessary to fuse interconnections prepared using thickened Ag pastes.

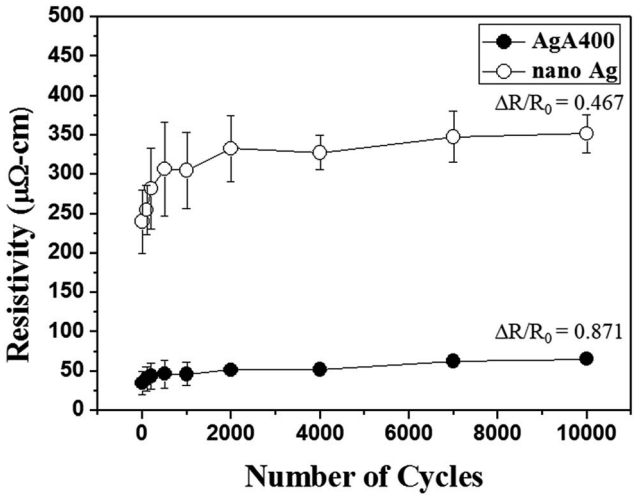

Fig. 11 Variation in electrical resistivity of AgA400 deposits and commercial nano-Ag pastes on PET subjected to different bending cycles after isothermally heated at 100 °C for 10 min (bending radius = 4.5 mm, bending frequency = 2 Hz).

the resistivity of commercial nano-Ag pastes cured under the same conditions. Fig. 11 also illustrates the change in electrical resistivity for 100 °C-cured AgA400 and nano-Ag deposits on PET substrate subjected to bending cycles. For both samples the electrical resistivity increased during the first 500 cycles and then slowed down up to 10 000 cycles. Subsequent to 10 000 bending cycles the resistivity of Ag SMP deposits increased from 35 to 65.5 μΩ cm ($\Delta R/R_0 = 0.87$), while that of commercial nano-Ag deposits increased from 240 to 352 μΩ cm ($\Delta R/R_0 = 0.47$). This suggests that low temperature-sintered SMP conductive films exhibit good bending fatigue resistance.

The morphologies of the sintered deposits subjected to 10 000 bending cycles are illustrated in Fig. 12. Both the sintered films were well attached on PET substrates without apparent peeling off or detachment. However, some strip-like loose regions can be found in the sintered nano-Ag, and no such regions were observed for sintered AgA400. This somehow

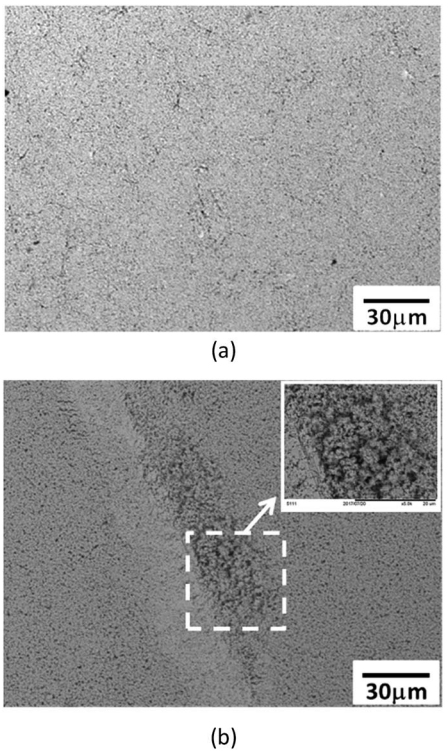

Fig. 12 Surface morphologies of sintered films on PET subjected to 10 000 bending cycles: (a) AgA400, and (b) nano Ag.

explain the inferior electrical conductance of nano-Ag compared with AgA400 subjected to sintering at 100 °C. Undesorbed surfactants which were trapped in the sintered deposits (as shown in Fig. 9(c)) caused structural loosening and thus lower electrical conductance.

4. Summary

In summary, a low temperature spray pyrolysis process for submicron Ag particles with an average diameter around 240–255 nm was developed in this study. Silver acetate with a decomposition temperature ranging from 200 °C to 265 °C was used as the precursor. Based on the results, a critical temperature existed between 350 to 400 °C for the full conversion of silver acetate into Ag powders. A small amount of residual precursors, 2.3 wt% in the case of spray pyrolysis at 350 °C, did not affect the electrical properties too much. Low temperature heating at 100 °C for 10 minutes can turn the Ag SMP pastes into excellent conductors, which can endure critical current density higher than 1 mA μm^{-2} under constant voltage of 12 V. The bending test results verify that 100 °C-sintered SMP conductive films on PET substrate exhibited good mechanical fatigue resistance.

Conflicts of interest

There are no conflicts to declare.

Acknowledgements

This work was supported by Ministry of Science and Technology of R. O. C. through the contract No. MOST 104-2628-E-005-001-MY2 and MOST 105-2119-M-006-008 for which the authors are grateful.

Notes and references

1 C. W. Chiu, P. D. Hong and J. J. Lin, *Langmuir*, 2011, **27**, 11690.
2 K. Okuyama and I. W. Lenggoro, *Chem. Eng. Sci.*, 2003, **58**, 537.
3 J. H. Bang and K. S. Suslick, *Adv. Mater.*, 2010, **22**, 1039.
4 S.-Y. Yang and S.-G. Kim, *Powder Technol.*, 2004, **146**, 185.
5 B. Ebin, E. Yazici and S. Gurmen, *Trans. Nonferrous Met. Soc. China*, 2013, **23**, 841.
6 X. Shi, S. Wang, X. Duan and Q. Zhang, *Mater. Chem. Phys.*, 2008, **112**, 1110–1113.
7 R. Zhang, X. Guo and H. Fu, *J. Appl. Surf*, 2011, **257**, 2367.
8 H. Lu, *Powder Technol.*, 2010, **203**, 176.
9 N. Kieda and G. L. Messing, *J. Mater. Res.*, 1998, **13**, 1660–1665.
10 S. J. Shih and I. C. Chien, *Powder Technol.*, 2013, **237**, 436–441.
11 K. Zhang, G. Peabody and E. Blankenhorn, *J. Mater. Res.*, 2013, **28**, 2753.
12 D. S. Jung, H. M. Lee, Y. C. Kang and S. B. Park, *J. Colloid Interface Sci.*, 2011, **364**, 574.
13 N. Kumar, F. Alam and V. Dutta, *J. Alloys Compd.*, 2014, **585**, 312.
14 S. J. Shih, W. L. Tzeng, R. Jatnika, C. J. Shih and K. B. Borisenko, *J. Biomed. Mater. Res., Part B*, 2015, **103**, 899.
15 Y. Hu, Y. Shi, H. Jiang, G. Huang and C. Li, *ACS Appl. Mater. Interfaces*, 2013, **5**, 10643.
16 N. L. Tarwal and P. S. Patil, *Electrochim. Acta*, 2011, **56**, 6510.
17 S. I. Park, J. H. Ahn, X. Feng, S. Wang, Y. Huang and J. A. Rogers, *Adv. Funct. Mater.*, 2008, **18**, 2673.
18 R. Dannenberg, E. Stach, J. R. Groza and B. J. Dresser, *Thin Solid Films*, 2000, **379**, 133.
19 T. Bakhishev and V. Subramanian, *J. Electron. Mater.*, 2009, **38**, 2720.
20 Y. S. Li, Y. C. Lu, K. S. Chou and F. J. Lin, *Mater. Res. Bull.*, 2010, **45**, 1837.